

14,15

## On the influence of strain rate on the nature of fracture in heterogeneous materials

© V.L. Hilarov, E.E. Damaskinskaya

Ioffe Institute,  
St. Petersburg, Russia

E-mail: Vladimir.Hilarov@mail.ioffe.ru

Received February 6, 2024

Revised February 6, 2024

Accepted February 7, 2024

The influence of mechanical loading rate on the nature of destruction of heterogeneous materials was studied using the discrete element method. With increasing impact speed, brittle-ductile and ductile-brittle transitions were discovered. Possible mechanisms of the influence of loading speed on the strength and nature of destruction of materials are discussed.

**Keywords:** fracture, strength of heterogeneous materials, loading speed, discrete element method.

DOI: 10.61011/PSS.2024.04.58209.18

The mechanical properties of materials significantly depend on the velocity of mechanical impact. The phenomenon of ductile-brittle transition at high material loading rates or temperature changes is well known, in particular the brittle behavior of liquids under impact [1].

Recently, there has been evidence of the existence of an inverse brittle-ductile transition at ultrahigh impact velocities of  $\sim 1-10$  km/s [2-5]. Such effects can be observed in collisions of spacecraft with micrometeorites, therefore, the study of such phenomena appears to be quite relevant.

The mechanism of the impact of the loading rate on strength is still unclear.

The behavior of a model heterogeneous material in case of its mechanical deformation at different velocities is studied in this paper. Calculations using the discrete element method (DEM) were performed in the freely distributable software package MUSEN [6].

The experimental design considered in this paper is similar to the design described in Ref. [7]. The sample comprises a cylinder with a diameter of 10 mm and a height of 20 mm. The cylinder is filled with grains (particles) with diameters and percentage composition as specified in Table 1 (a particle diameter in millimeters, their quantity 48695). This is a set of sizes with a mean value of 0.3 mm and a standard deviation of 0.1 mm which was obtained by a normal random number generator. Particles of the same material were bonded by the same material while heterogeneous particles were coupled by low-modulus bonds 4-6 (Table 2). Bond diameters is  $d \leq 0.6$  mm. Thus, the well-known bonded particle model (BPM) was implemented [8].

The sample was placed in a virtual press in which the lower plate was fixed, and the upper plate moved in the direction of the lower plate at the speeds of  $v = 0.02-5000$  m/s until the samples were destroyed. The fracture process, in equal time periods — a data saving time

interval — recorded a large set of data of various mechanical parameters of the sample, which could be used for further analysis. The force with which the sample acts on the upper plate, and the number of broken bonds of each type, as well as the total number of broken bonds were such parameters in this study.

Figure 1 shows the sample fracture patterns at different plate displacement velocities.

**Table 1.** Grain diameters (mm) and percentage composition of each of the fractions

Material	Diameter of grains of different fractions $d_i$ , mm					Proportion of each fraction
	0.36	0.188	0.52	0.28	0.42	
Quartz	0.36	0.188	0.52	0.28	0.42	0.0595745
Orthoclase	0.27	0.28	0.4	0.36	0.26	0.0702128
Oligoclase	0.16	0.168	0.288	0.24	0.4	0.0702127

**Table 2.** Parameters of materials used for simulation

Nº	Material	$\rho$ , kg/m <sup>3</sup>	$E$ , GPa	$\nu$	$\sigma_n$ , MPa	$\sigma_t$ , MPa	$\eta$ , Pa·s
1	Quartz	2650	94	0.29	600	600	5E19
2	Orthoclase	2560	62	0.29	420	420	1E19
3	Oligoclase	2560	70	0.29	480	480	1E19
4	Quartz-orthoclase bond	2500	5.8	0.2	200	200	5E19
5	Quartz-oligoclase bond	2500	5.8	0.2	300	300	5E19
6	Orthoclase-oligoclase bond	2500	5.8	0.2	100	100	5E19

Note.  $\rho$  is the material density,  $E$  is the Young's modulus,  $\nu$  is the Poisson's ratio,  $\sigma_n$  is the material tensile strength,  $\sigma_t$  is the shear strength of the material,  $\eta$  is the dynamic viscosity.

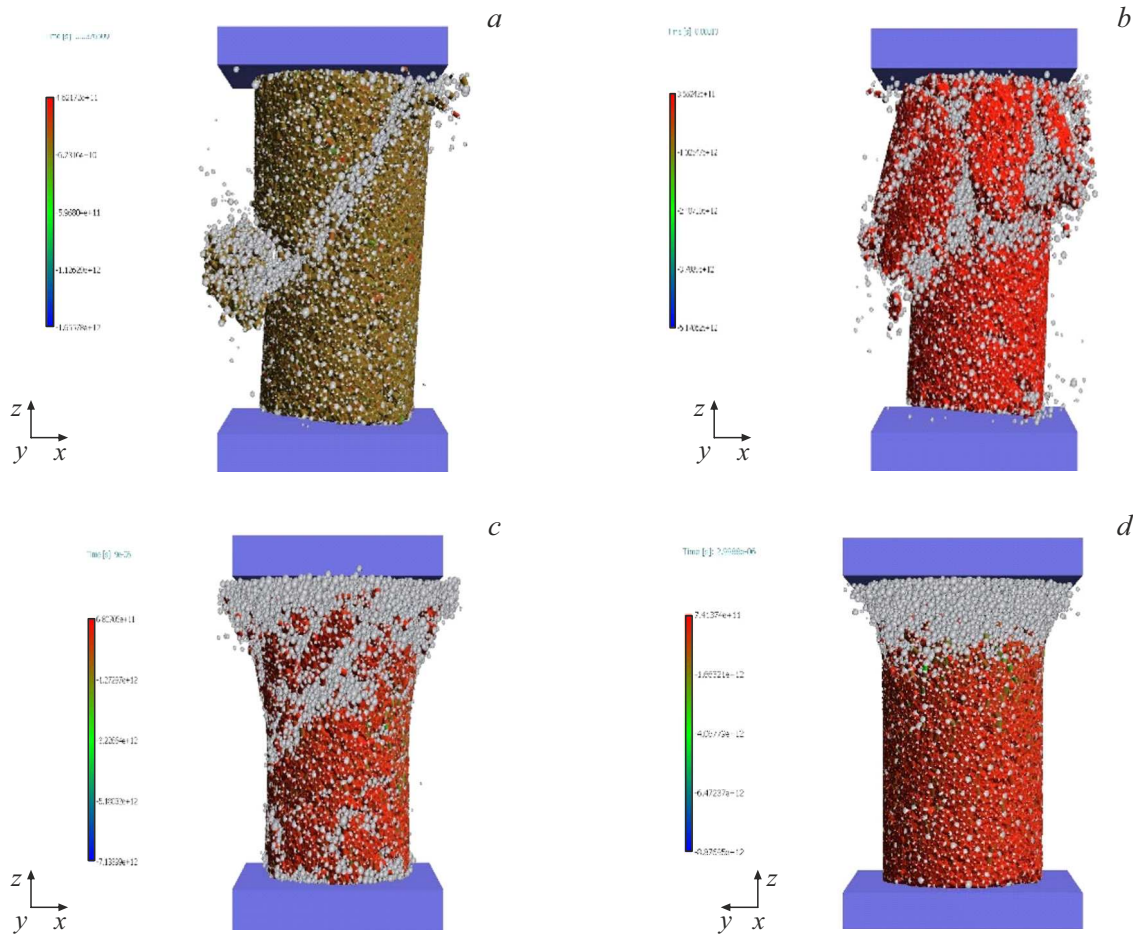


**Figure 1.** Sample fracture patterns at different plate displacement velocities: *a*)  $v = 0.02 \text{ m/s}$ ; *b*)  $v = 10 \text{ m/s}$ ; *c*)  $v = 500 \text{ m/s}$ ; *d*)  $v = 1000 \text{ m/s}$ . The color indicates the normal stresses on the bonds.

It is apparent that the fracture patterns significantly differ at low and high loading rates. One crack is formed at a loading rate of  $0.02 \text{ m/s}$  (Figure 1, *a*) and the sample splits into several fragments at a higher loading rate ( $10 \text{ m/s}$  — Figure 1, *b*). Figure 1, *c* ( $v = 500 \text{ m/s}$ ) demonstrates a mixed fracturing character: a crack appears, similar to the one shown in Figure 1, *a*, and there is also intense fracturing (bonds are broken) near the moving plate. The material crumbles in front of the moving plate at a loading rate of  $1000 \text{ m/s}$  (Figure 1, *d*).

Figure 2 shows the time dependence of the force acting from the material on the upper plate. This characteristic is an equivalent of the material loading diagram. Figure 2, *a* corresponds to the material fracturing preceded by plastic deformation (plateau on the dependence). The time domain of plastic deformation is much smaller both on an absolute and relative scale in Figure 2, *b*. Therefore, the embrittlement of the material takes place in this velocity range. A nonlinear region (equivalent of plasticity) reappears on the force diagram, as well as a yield drop in Figure 2, *c*. Its occurrence can be explained by the fact that at such high velocities the material relaxes with some lag relative to the

load. Figure 2, *d* illustrates the case when bond strength no longer plays a role, and the resistance of the material to the load is determined by the inertial component [5].

Indeed, the barrier penetration resistance  $P$  can be represented as the sum of the strength ( $R$ ) and inertial ( $1/2\rho v^2$ ) components according to [5] (1):

$$P = \frac{1}{2}\rho v^2 + R, \quad (1)$$

where  $\rho$  is the material density,  $v$  is the penetration rate. The inertial component is nothing more than the resistance of the ductile medium to the movement of the loading plate. The plate interacts with practically intact material, which crumbles under it as a loose medium at high velocities  $v$ , above the velocity of the fracture front. The growth of force at the end of the diagram in Figure 2, *d* is associated with the impact of the upper plate on the lower one.

Thus, we first observe a well-known ductile-brittle transition with an increase of the loading rate, and on the contrary, the transition is brittle-ductile at higher velocities.

A comparison of the values of the maximum force acting on the plate (equivalent of the ultimate strength of the

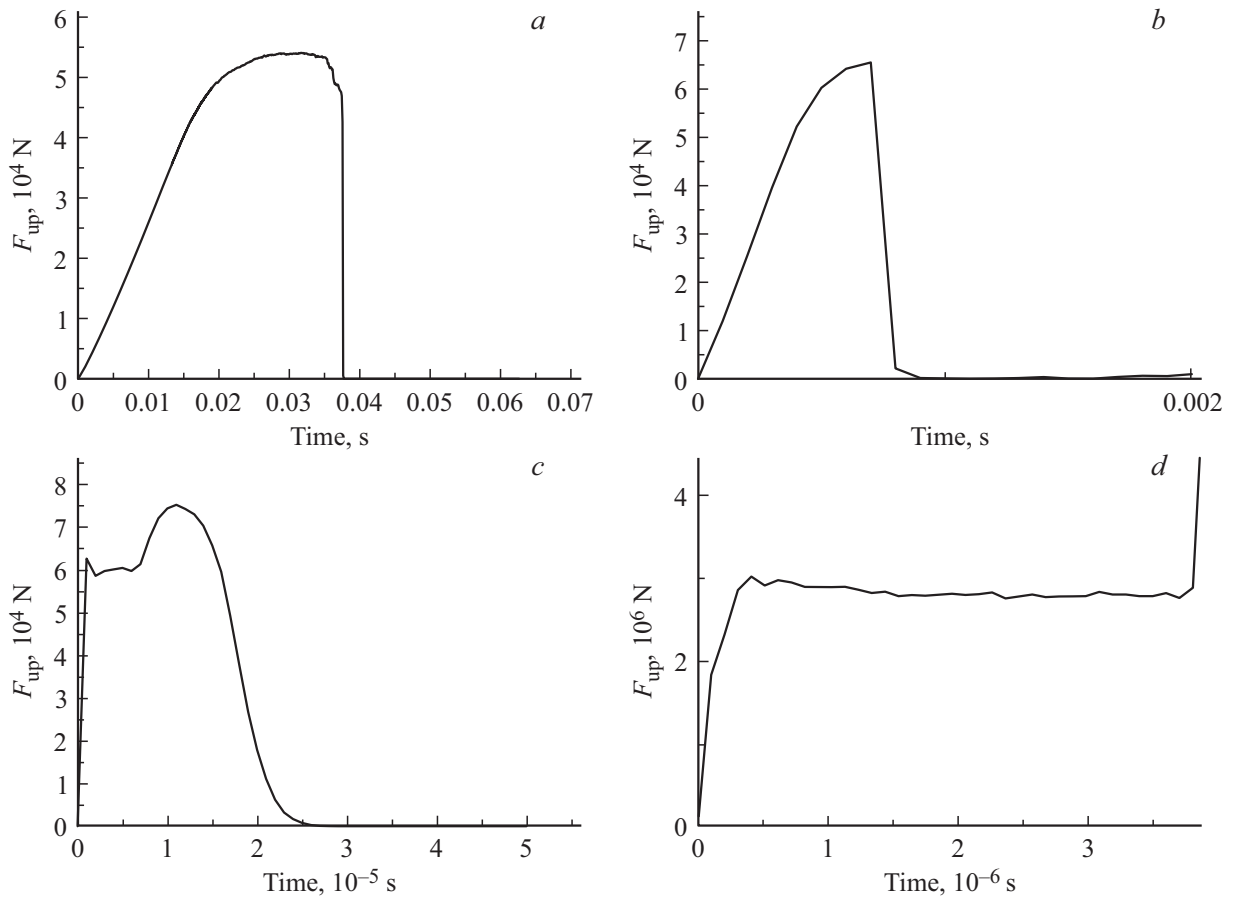


**Figure 2.** Dependence on the time of the total force acting from the side of the sample on the upper plate moving at different velocities: a)  $v = 0.02 \text{ m/s}$ ; b)  $v = 1 \text{ m/s}$ ; c)  $v = 100 \text{ m/s}$ ; d)  $v = 5000 \text{ m/s}$ .

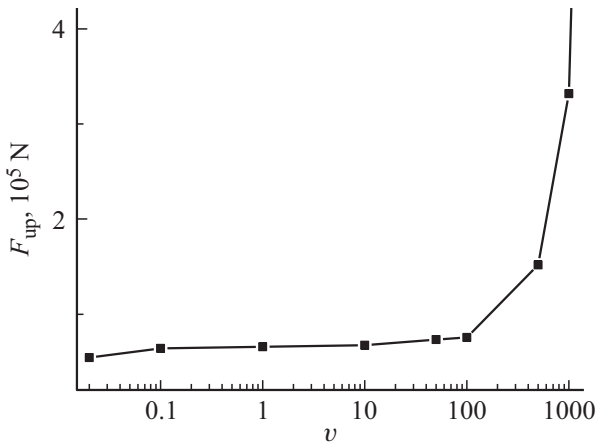


**Figure 3.** Dependence of the maximum force acting on the plate on its velocity.

material) shows that this value increases with the increase of the plate velocity. Figure 3 shows the dependence of the maximum force on the velocity.

It should be noted that a similar dependence of strength on velocity was obtained by model calculation in the ap-

proximation of „incubation time“ in Ref. [9]. Experimental strength data of structural steel A are also provided and a good agreement of model and experimental results is shown.

It is possible to trace the fracturing of individual elements of the structure for understanding the reasons of the increase of the strength of the material with an increase of the impact rate in DEM. Such elements are bonds between particles in the BPM. Figure 4, a shows the total number of bonds broken by the sample destruction point. The destruction point is considered to be the moment in time when the force on the upper panel decreases to almost zero (Figure 2, a–c). A pronounced crack is formed in this case (Figure 1, a–c). The sample crumbles under the plate at higher velocities as already noted (Figure 1, d), and its loading diagram (the force acting on the upper plate) remains approximately constant in time (Figure 2, d).

The total number of bonds broken by the destruction point decreases at loading rates which are not very high (Figure 4, a). It follows from Figure 4, b that in this case, the bonds consisting of the same material as the particles of the same material coupled by these bonds are first broken, which can be interpreted as intragranular fracture. „Intergranular“ bonds remain mostly intact, since they are deformable due to the low modulus of elasticity.

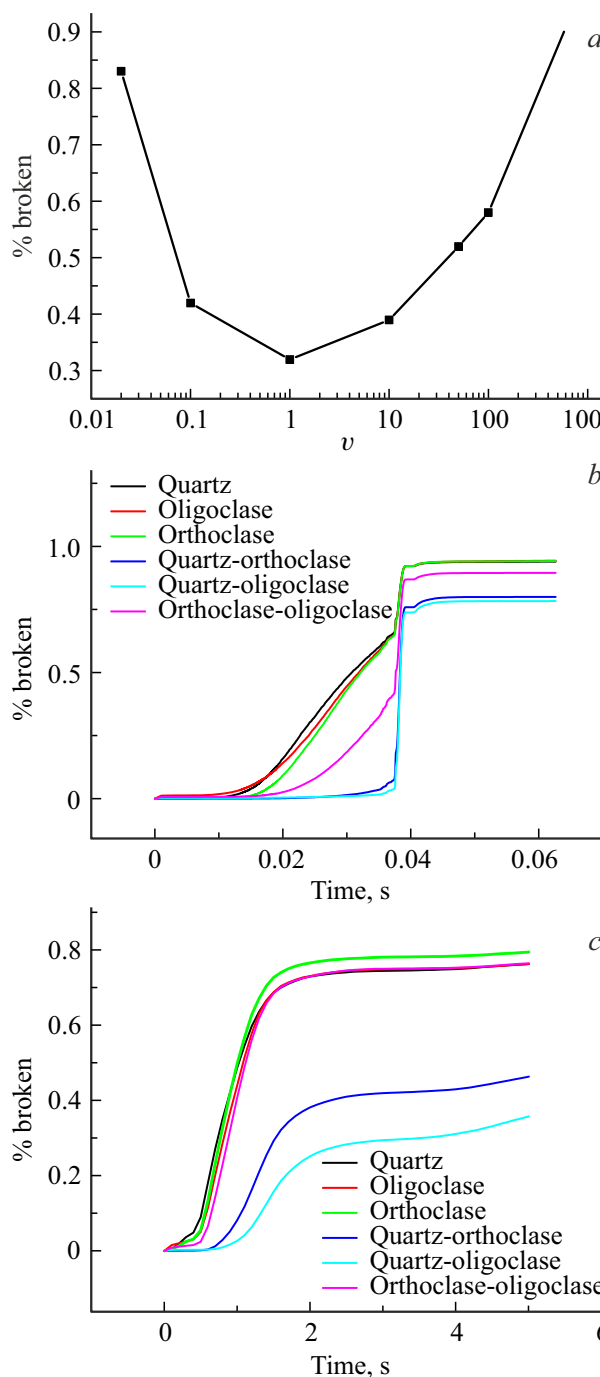


**Figure 4.** *a* — the total number of broken bonds by the time of sample fracturing; *b* — the kinetics of bond breakage from each material at a velocity of  $v = 0.02$  m/s; *c* — the kinetics of bond breakage from each material at a velocity of  $v = 100$  m/s.

The rupture of the „intragranular“ bonds ensures the quasi-plasticity of the considered material manifested in the „loading diagram“ (Figure 2, *a*). The lagging in breakage of the „intergranular“ and „intragranular“ bonds decreases with an increase of the loading rate (Figure 4, *c*). This results in the embrittlement of the material — a ductile-brittle transition takes place. At the same time, the total

number of broken bonds (Figure 4, *a*) decreases, which, in our opinion, results in an increase of the strength of the material in this velocity range.

The contribution of the inertial component to the fracture resistance of the sample increases with a further increase of the loading rate. As already noted, the material begins to crumble under the loading plate. The number of broken bonds increases by the destruction point (Figure 4, *a*). A shelf characteristic of plasticity is formed on the „loading diagram“ (Figure 2, *c*). The reverse brittle-ductile transition takes place. The increase of the strength of the material in this velocity range can be explained by an increase of the inertial contribution in expression (1).

Thus, the destruction of a heterogeneous sample at different rates of mechanical impact was considered using the discrete element method. The use of computer modeling made it possible to identify the main fracture patterns on the same sample, i.e., to deliberately exclude any impact of variations of the structure of the material. It was shown that a ductile-brittle transition first occurs in the material with an increase of the impact rate because all the bonds in the system begin to collapse simultaneously at these rates. At higher rates, a brittle-ductile transition is observed in the system, associated with an increase of the contribution of the inertial component to the strength.

It should be noted that the numerical values of the quantities obtained in this study for the model material cannot be directly compared with the results of a laboratory experiment, because physical parameters used in the DEM were not calibrated which is necessary for such a comparison.

## Conflict of interest

The authors declare that they have no conflict of interest.

## References

- [1] M. Kornfeld. Uprugost' i prochnost' zhidkostej. Gos. Izd. Tekh.-Teor. Lit., M.-L. (1951). 109 p. (in Russian).
- [2] A.A. Kozhushko, I.I. Rykova, A.B. Sinani. Fizika gorenija i vzryva, 1 89, (1992). (in Russian).
- [3] V.B. Lazarev, A.S. Balankin, A.D. Izotov, A.A. Kozhushko. Strukturnaya ustochivost' i dinamicheskaya prochnost' ne-organicheskikh materialov. Nauka, M. (1993). P. 175. (in Russian).
- [4] E.I. Zilberbrand, A.S. Vlasov, J.U. Cazamias, S.J. Bless, A.A. Kozhushko. Int. J. Impact Eng. **23**, 1, 995 (1999).
- [5] A.A. Kozhushko, A.B. Sinani. FTT **47**, 5, 812 (2005). (in Russian).
- [6] M. Dosta, V. Skorych. Software X **12**, 100618 (2020).
- [7] V.L. Hilarov, E.E. Damaskinskaya. FTT **64**, 676 (2022). (in Russian).
- [8] D.O. Potyondy, P.A. Cundall. Int. J. Rock Mech. Min. Sci. **41**, 1329 (2004).
- [9] A.D. Evstifeev, A.A. Gruzdkov, Yu.V. Petrov. ZhTF **83**, 7, 59 (2013). (in Russian).

Translated by A.Akhtyamov